

Zero field splitting parameter and energy levels of Mn^{2+} in $LiAl_5O_8$ single crystals

Maroj Bharati ^a, Vikram Singh ^a, Ram Kripal ^b

^a Department of Physics, Nehru Gram Bharti (DU), Jamunipur, Prayagraj, India

^b EPR Laboratory, Department of Physics, University of Allahabad, Prayagraj-211002, India

Abstract

The Mn^{2+} doped $LiAl_5O_8$ single crystals' crystal field parameters and zero-field splitting parameter are theoretically determined utilizing the perturbation theory and the superposition model. The experimental value and the theoretical zero-field splitting parameter D are in good agreement. This establishes the experimental outcome that Mn^{2+} ions substitute at Li^+ site in $LiAl_5O_8$ single crystal. The optical spectra of Mn^{2+} doped $LiAl_5O_8$ crystal are computed using the crystal field parameters and the crystal field analysis computer program. The computed and empirical energy values match reasonably well. Hence the theoretical study backs the experimental one.

Keywords: A. Inorganic compounds; A. Single crystal; D. Crystal fields; D. Optical properties; D. Electron paramagnetic resonance.

Date of Submission: 28-08-2024

Date of Acceptance: 07-09-2024

I. Introduction

Transition ion local site symmetry in doped crystals and distortions taking place in the lattice are obtained by electron paramagnetic resonance, or EPR [1-3]. According to these research, transition ion (d^5) spin Hamiltonian parameters (SH) are quite sensitive to local distortions. The SH parameters may be correlated with optical and structural parameters employing microscopic spin-Hamiltonian (MSH) theory.

The crystal-field (CF) parameters of d^5 ion may be obtained by superposition model (SPM) [4, 5]. The CF parameters can be used afterwards to determine the zero field splitting (ZFS) parameters [6]. Mn^{2+} ion has $^6S_{5/2}$ ground state [7-9] and hence is quite interesting.

Lithium aluminates have been paid attention recently due to their several industrial applications. These compounds show excellent radiation and thermochemical stability, making them useful as blanket subjected to radiation in nuclear fusion reactors and on ceramic matrices in fuel cells that use molten carbonate [10–11]. Apart from these, they behave as good materials that glow when doped with impurities [12–13]. Many studies on $LiAlO_2$ have been documented [14–16] but there is little report on $LiAl_5O_8$. $LiAl_5O_8$ having an inverse spinel structure shows intriguing optical characteristics. The important factor in the optical characteristics of these substances is the characteristic of dopants.

Fe^{3+} luminescence in lithium aluminate has been largely reported [17–18] as Fe^{3+} doping gives red emitting phosphors useful for artificial illumination in various applications. $LiAl_5O_8$ doped with Eu or Co are also reported [13, 19, 20] as these also yield efficient luminescence. Mn^{2+} ions exhibit green, orange, and red photoluminescence under UV irradiation in most host materials and are, hence, largely used as phosphors for lamps and displays [21–22].

EPR study of Mn^{2+} doped lithium aluminate ($LiAl_5O_8$) single crystal at 300 K has been performed [23]. The present investigation evaluates the CF parameters using SPM and these parameters with MSH theory provide ZFS parameter for Mn^{2+} ions at the axial center in $LiAl_5O_8$ single crystal at 300 K. The experimental and theoretical ZFS parameter D match well [23].

II. Crystal Structure

At 300K $LiAl_5O_8$ crystallizes in a space group $P4_332$ -containing inverse spinel structure. The constant of lattice $a = 7.908 \text{ \AA}$ and $Z = 4$ [24] (Fig. 1). Two kinds of coordination polyhedra around Li^+ and Al^{3+} ions (tetrahedrons and octahedrons) are shown. Kordes [25] suggested both the primitive cubic and spinel structure for $LiAl_5O_8$, wherein Li^+ and a portion of Al^{3+} jointly occupied both octahedral and tetrahedral position. After doping Mn^{2+} ions substitute for Li^+ ions with charge compensation. Mn^{2+} ions show preference to substitute for Li^+ ions in the tetrahedral sites [23]. The site symmetry in the vicinity of Mn^{2+} ions may be taken to be axial, as indicated by EPR investigation of Mn^{2+} in $LiAl_5O_8$ [23].

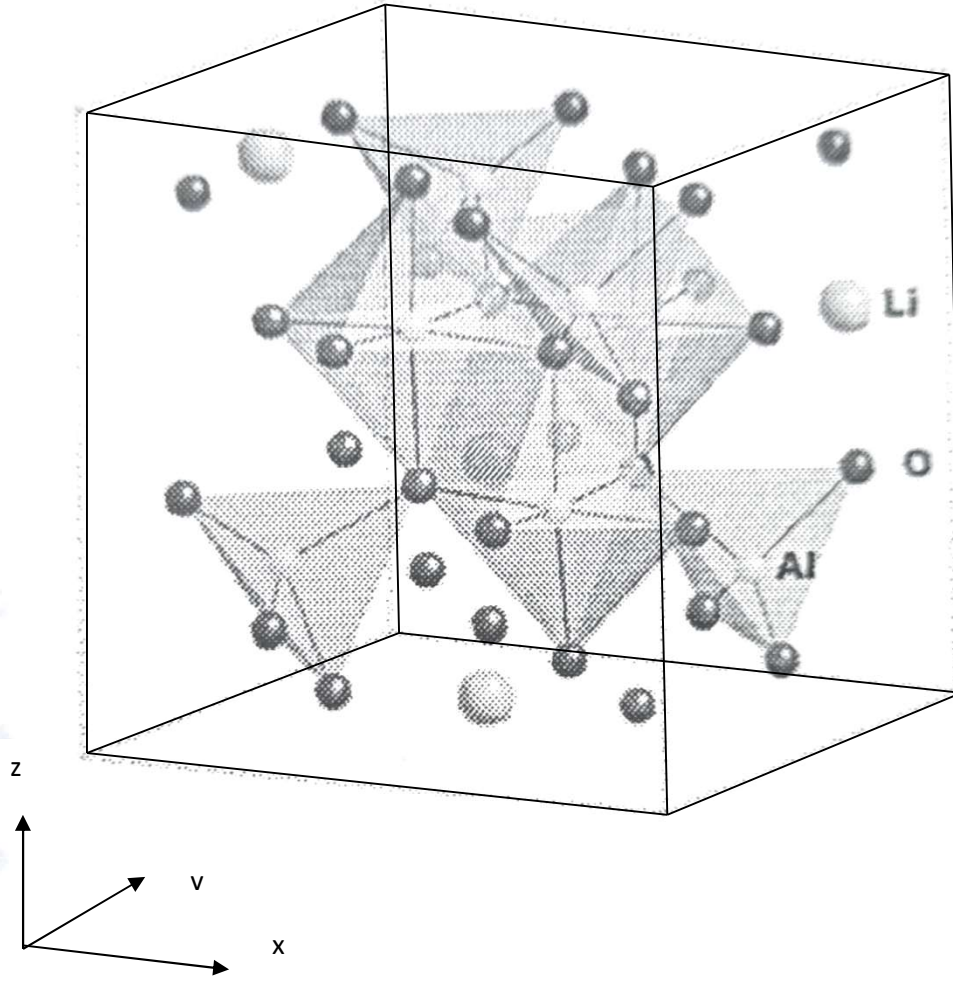


Fig. 1: Crystal structure of $LiAl_5O_8$ together with axes (SAAS-symmetry adopted axes system).

III. Theoretical Investigation

The SH of $3d^5$ ion in axial symmetry crystal field is given

$$\begin{aligned} \mathcal{H} = & g \mu_B B.S + D \left\{ S_z^2 - S(S+1) \right\} + \left(\frac{a}{6} \right) \left[S_x^4 + S_y^4 + S_z^4 - \frac{1}{5} S(S+1) (3S^2 + 3S - 1) \right] \\ & + \frac{F}{180} \left\{ 35 S_z^4 - 30 S(S+1) S_z^2 + 25 S_z^2 - 6 S(S+1) + 3 S^2 (S+1)^2 \right\} \\ & + A(I.S) \end{aligned} \quad (1)$$

where the initial term gives electronic Zeeman interaction, B is the external magnetic field, the Bohr magneton is represented by μ_B , and g is the spectroscopic splitting factor. The second-rank axial, fourth-rank cubic, and fourth-rank axial ZFS terms are the second, third, and fourth terms, respectively [8]. The hyperfine interaction

term is the fifth term. The letters S, D, *a*, and F denote the effective spin vector, second order axial, fourth-rank cubic, and fourth-rank axial ZFS parameters, respectively. The electronic Zeeman interaction is considered to be isotropic for Mn²⁺ ions [8, 29, 30].

For a d⁵ ion, the Hamiltonian is given as

$$\mathcal{H} = \mathcal{H}_0 + \mathcal{H}_{cf} + \mathcal{H}_{so}$$

where $\mathcal{H}_{cf} = \sum_{kq} B_{kq} C_q^k$ (2)

is the Hamiltonian of the crystal field while \mathcal{H}_{so} and \mathcal{H}_0 are spin-orbit (SO) coupling and the unbound ion Hamiltonian, respectively. Since the spin-spin coupling is quite small [31-33], its contribution is neglected in Eq. (2). The perturbation term is the field of the SO interaction [34-36]. The ZFS parameter D's SO contribution for 3d⁵ ions in axial symmetry is provided as [35]

$$D^{(4)}(SO) = \left(\frac{\xi^2}{63 P^2 G} \right) [14 B_{44}^2 - 5 B_{40}^2] - \left(\frac{3 \xi^2}{70 P^2 D} \right) B_{20} [B_{20} - 14 \xi] \quad (3)$$

where $P = 7(B+C)$, $G = 10B+5C$ and $D = 17B+5C$. P, G, and D yield the energy differences between the ground sextet and the excited quartets. The Racah parameters B and C represent the electron-electron repulsion. In Eq. (3), only the fourth order term is included since the other perturbation terms are negligible [35, 36]. $B = N^4 B_0$, $C = N^4 C_0$, and $\xi = N^2 \xi_0$ represent the parameters B, C, and ξ in terms of the average covalency parameter N, where B_0 , C_0 , and ξ_0 are the Racah parameters and the spin-orbit coupling parameter for free ion, respectively [37]. $B_0 = 960 \text{ cm}^{-1}$, $C_0 = 3325 \text{ cm}^{-1}$, $\xi_0 = 336 \text{ cm}^{-1}$ are taken here [8] for free Mn²⁺ ion. Using equation

$$N = \left(\sqrt{B/B_0} + \sqrt{C/C_0} \right) / 2 \quad (4)$$

N is evaluated taking the values of Racah parameters ($B = 917 \text{ cm}^{-1}$, $C = 2254 \text{ cm}^{-1}$) from optical absorption of Mn²⁺ ion in crystal where there are oxygen ligands [38].

ZFS parameter D is determined from Eq. (3) after CF parameters for Mn²⁺ in LiAl₅O₈ single crystal are established from SPM. A comparable method has been considered for obtaining ZFS parameters by various other workers [39].

To interpret the crystal-field splitting in different crystals, the SPM is generally used. The model mentioned above has also been utilized for 3dⁿ ions [40]. The parameters of the crystal field B_{kq} , using above model, are evaluated from the equations [41]:

$$B_{20} = -2 \bar{A}_2 \left(\frac{R_0}{R_{10} + \Delta R_1} \right)^{t_2} - 4 \bar{A}_2 \left(\frac{R_0}{R_{20} + \Delta R_2} \right)^{t_2} \quad (5)$$

$$B_{40} = 16 \bar{A}_4 \left(\frac{R_0}{R_{10} + \Delta R_1} \right)^{t_4} + 12 \bar{A}_4 \left(\frac{R_0}{R_{20} + \Delta R_2} \right)^{t_4} \quad (6)$$

$$B_{44} = 2\sqrt{70} \bar{A}_4 \left(\frac{R_0}{R_{20} + \Delta R_2} \right)^{t_4} \quad (7)$$

where R_0 is the reference distance, typically calculated as the axially symmetric mean of the four bond lengths.

ΔR_1 and ΔR_2 provide the distortion parameters. \bar{A}_2 , \bar{A}_4 and t_k represent the intrinsic parameters and power law exponent,

IV. Results and Discussion

The position of Mn²⁺ ion and spherical polar coordinates of ligands are displayed in Table 1. Two of the four Mn²⁺-O²⁻ bond lengths have an average value of $R_{10} = 0.5540 \text{ nm}$, and the remaining two have an average value

of $R_{20} = 0.5880$ nm, respectively. In tetrahedral coordination, $\overline{A_4}(R_0) = (-27/16)Dq$ [6]. The ratio $\frac{\overline{A_2}}{\overline{A_4}}$ for $3d^5$ ions lies between 8 and 12 [40]. For the Mn^{2+} ion, the power law exponent is found to be $t_2 = 3$, $t_4 = 7$. To obtain the values of intrinsic parameters in SPM, semi-ab initio analysis for other transition ions are done; the same method is employed here.

Table 1 Atomic coordinates in LiAl₅O₈ crystal and spherical polar coordinates of ligands R θ , ϕ .

Position of Mn ²⁺ (Fractional)	Ligands			Spherical co-ordinates of ligands			
				R(nm)	θ^0	ϕ^0	
	x	y	z		(degree)		
	(Å)						
Site : Substitutional	O1	0.1146	0.1329	0.3847	0.3373	24.82	49.14
Li	O2	0.3859	0.3859	0.3859	0.5320	54.74	45.00
(-0.0025, -0.0025, -0.0025)	O3	0.6146	0.3671	-0.3847	0.6441	117.98	30.91
	O4	0.8859	0.1141	-0.3859	0.7707	113.16	7.47

B, C, and Dq values are determined from study of optical absorption [38] as 917, 2254 and 756 cm⁻¹, respectively. First no local distortion is considered and D's value is computed. This can be done by taking $\frac{\overline{A_2}}{\overline{A_4}} = 10$ and $R_0 = 0.211$ nm, which is a bit less than the total ionic radii of $Mn^{2+} = 0.083$ nm and $O^{2-} = 0.140$ nm, there are the B_{kq} parameters as: $B_{20} = 3766.596$ cm⁻¹, $B_{40} = -35.4417$ cm⁻¹, $B_{44} = -16.3424$ cm⁻¹ and D's value as: $|D| = 5.3 \times 10^{-4}$ cm⁻¹. EPR study yields the D experimental value as: $|D| = 299.0 \times 10^{-4}$ cm⁻¹ [23]. The experimental value is found to be greater than the theoretical value from above.

Now, taking local distortions as $\Delta R_1 = -0.18780$ nm and $\Delta R_2 = -0.18770$ nm, $R_0 = 0.211$ nm and ratio $\frac{\overline{A_2}}{\overline{A_4}} = 10$,

Table 2 shows the calculated B_{kq} parameters and the D as: $|D| = 299.2 \times 10^{-4}$ cm⁻¹, in excellent conformity with the experimental value: $|D| = 299.0 \times 10^{-4}$ cm⁻¹. Taking B_{kq} parameters and CFA program [42-43], the optical spectra of Mn^{2+} doped LiAl₅O₈ single crystal are computed. The energy levels of Mn^{2+} ion are calculated by diagonalizing the complete Hamiltonian within the $3d^N$ basis of states in the intermediate crystal field coupling scheme. Table 3 presents the calculated energy values (input parameters are given below the Table) along with the experimental values [38] for comparison. It is noted from Table 3 that the computed and experimental energy values are reasonably in agreement. The energy values evaluated without considering distortion were quite different from the experimental ones and so are not being given here. Hence the theoretical study backs the experimental investigation.

Table 2. Crystal field parameters and zero field splitting parameters of Mn^{2+} doped LiAl₅O₈ single crystal.

ΔR_1 (nm) ΔR_2 (nm) R_0 (nm)			Crystal- field parameters (cm ⁻¹)			Zero-field splitting parameter (10 ⁻⁴ cm ⁻¹)
			B_{20}	B_{40}	B_{44}	$ D $

- 0.18780	-0.18770	0.211	12254.79	-1124.96	-98.449	299.2
0.00000	0.00000	0.211	3766.596	-35.4417	-16.3424	5.3
Exptl.						299.0

Table 3. Experimental and calculated (CFA package) energy band positions of Mn²⁺ doped LiAl₅O₈ single crystal.

Transition from ⁶ A _{1g} (S)	Observed energy bands (cm ⁻¹)	Calculated energy bands (cm ⁻¹) With distortion
⁴ T _{1g} (G)	16044	19708, 19923, 20045, 20049, 20175, 20195
⁴ T _{2g} (G)	20433	20240, 20293, 20333, 20456, 20481, 20558
⁴ E _g (G)	24108	21965, 21969, 22383, 22403
⁴ A _{1g} (G)	24242	25586, 25640
⁴ T _{2g} (D)	26724	25729, 25812, 27283, 27324, 28115, 28190
⁴ E _g (D)	30451	30326, 30426, 30527, 30633
⁴ T _{1g} (P)	33956	33709, 33845, 34097, 34296, 34519, 34590
⁴ A _{2g} (F)	36846	36770, 36868
⁴ T _{1g} (F)	38521	38464, 38556, 38618, 38639, 38689, 38691

Input parameters: Numbers of free ion parameters = 5, number of d shell electrons = 5, number of fold for rotational site symmetry = 1; Racah parameters in A, B and C, spin-orbit coupling constant and Trees correction are 0, 917, 2254, 336 and 76 cm⁻¹, respectively; number of crystal field parameters = 3; B₂₀, B₄₀, B₄₄ are taken from Table 2, spin-spin interaction parameter, M0 = 0.2917; spin-spin interaction parameter, M2 = 0.0229; spin-other-orbit interaction parameter, M00 = 0.2917; spin-other-orbit interaction parameter, M22 = 0.0229; magnetic field, B = 0.0 Gauss; angle between magnetic field B and z-axis = 0.00 degree.

V. Conclusions

In LiAl₅O₈ single crystal, the superposition model and perturbation analysis have been used to calculate the zero-field splitting parameter D for Mn²⁺. The theoretical D matches well with the experiment when distortion is introduced into calculation. The theoretical study indicates that the ion Mn²⁺ resides in Li⁺ site with charge compensation which validates the experimental EPR study's conclusions. It is observed from CF energy calculation that the calculated and experimental results have a fair degree of agreement. Hence the theoretical study supports the experimental results. The procedure employed here may be used to several other ion-host systems for exploring crystals of scientific and industrial applications.

ACKNOWLEDGEMENT

The writers express their gratitude to the Head, Department of Physics for providing the departmental facilities and to Prof. C. Rudowicz, Faculty of Chemistry, A. Mickiewicz. University, Poznan, Poland for CFA program.

References

- [1]. C. Rudowicz, S. K. Misra, Appl. Spectrosc. Rev. 36 (2001) 11.
- [2]. Z.Y. Yang, Y. Hao, C. Rudowicz, Y.Y. Yeung, J. Phys.: Condens. Matter 16 (2004) 3481.
- [3]. P. Gnutek, Z. Y. Yang, C. Rudowicz, J. Phys.: Condens. Matter 21 (2009) 455.

- [4]. S. K. Misra in: Handbook of ESR (Vol.2), eds. C. P. Poole Jr., H. A. Farach, Springer, New York, 1999, Chapter IX, p. 291.
- [5]. H. Anandlakshmi, K. Velavan, I. Sougandi, R. Venkatesan, P. S. Rao, Pramana 62 (2004) 77.
- [6]. S. Pandey, R. Kripal, A. K. Yadav, M. Açıkğöz, P. Gnutek, C. Rudowicz, J. Lumin. 230 (2020) 117548 (9 pages).
- [7]. I. Stefaniuk, Opto-Electronics Rev. 26(2018)81.
- [8]. A. Abragam, B. Bleaney, Electron Paramagnetic Resonance of Transition Ions, Clarendon Press, Oxford, 1970.
- [9]. D. J. Newman, B. Ng (Eds.), Crystal Field Handbook, Cambridge University Press, Cambridge, 2000.
- [10]. Y. Kawamura, M. Nishikawa, K. Tanaka, H. Matsumoto, J. Nucl. Sci. Technol. 29 (1992) 436.
- [11]. S. Terada, I. Nagashima, K. Higaki, Y. Ito, J. Power Sources 75 (1998) 223.
- [12]. T. Abritta, F. de Souza Barros, J. Lumin. 40/41 (1988) 187.
- [13]. L. Zuwu, L. Xi, L. Jun, Nat. Sci. J. Xiangtan. Univ. 18 (1996) 49.
- [14]. M.A. Valenzuela, J. Jimenez-Becerril, P. Bosch, S. Bulbulian, V.H. Lara, J. Am. Ceram. Soc. 79 (1996) 455.
- [15]. S.W. Kwon, E.H. Kim, S.B. Park, J. Mater. Sci. Lett. 18 (1999) 931.
- [16]. P. Ravindranathan, S. Komarneni, R. Roy, J. Mater. Sci. Lett. 12 (1993) 369.
- [17]. J. Maria Neto, T. Abritta, F. de Souza Barros, J. Lumin. 22 (1981) 109.
- [18]. J. G. Rabatin, J. Electrochem. Soc. 25 (1978) 920.
- [19]. T. Ishihara, T. Katsuhisa, H. Kazuyuki, S. Naohiro, in: J.D. Mackenzie (Ed.), Proceedings of the SPIE on Sol-Gel Optics III, vol. 2288, 1994 (Issue 10 p. 668).
- [20]. D. Xiulan, Y. Duorong, J. Non-Cryst. Solids 351 (2005) 2348.
- [21]. K. Kang, S.H. Huang, X.W. Huang, F.T. You, S.S. Zhang, H.Q. He, J. Lumin. 122/123 (2007) 804.
- [22]. T.S. Copeland, B.I. Lee, J. Qi, A.K. Elrod, J. Lumin. 97 (2002) 168.
- [23]. V. Singh, R. P. S. Chakradhar, J.L. Rao, D. K. Kim, Mat. Chem. Phys. 110 (2008) 43.
- [24]. R. Famery, F. Queyroux, J. C. Gilles, P. Herpin, J. Solid State Chem. 30 (1979) 257.
- [25]. E. Kordes, Zeits.fur. Krist. 91 (1935) 193.
- [26]. M. G. Zhao, M. L. Du, G. Y. Sen, J. Phys. C: Solid State Phys. 18 (1985) 3241.
- [27]. W. L. Yu, Phys. Rev. B 39 (1989) 622.
- [28]. Z. Y. Yang, J. Phys.: Condens. Matter 12 (2000) 4091.
- [29]. D. J. Newman, B. Ng, Rep. Prog. Phys. 52, (1989) 699.
- [30]. W. L. Yu, M. G. Zhao, Phys. Rev. B 37 (1988) 9254.
- [31]. Z. Y. Yang, C. Rudowicz, Y. Y. Yeung, Physica B 348 (2004) 151.
- [32]. C. Rudowicz, H. W. F. Sung, Physica B 300 (2001) 1.
- [33]. C. J. Radnell, J. R. Pilbrow, S. Subramanian, M. T. Rogers, J. Chem. Phys. 62 (1975) 4948.
- [34]. J. A. Weil, J. R. Bolton, Electron Paramagnetic Resonance: Elementary Theory and Practical Applications, second ed., Wiley, New York, 2007.
- [35]. W. L. Yu, M. G. Zhao, J. Phys. C: Solid State Phys., 18 (1984) L525.
- [36]. J. F. Clare, S. D. Devine, J. Phys. C: Solid State Phys., 17 (1984) L581.
- [37]. T. H. Yeom, S. H. Choh, M. L. Du, M. S. Jang, Phys. Rev. B 53(1996) 3415.
- [38]. R. Kripal, H. Govind, S. K. Gupta, M. Arora, Physica B 392(2007) 92.
- [39]. W. L. Yu, M. G. Zhao, Phys. Stat. B 140 (1987) 203.
- [40]. Y. Y. Yeung, Superposition model and its applications, in: Optical Properties of 3d-Ions in Crystals, Spectroscopy and Crystal Field Analysis (Chapter 3, pp.95-121), M. G. Brik and N. M. Avram (Eds.), Springer: Heidelberg, New York, Dordrecht, London, 2013.
- [41]. Q. Wei, Acta Phys. Polon. A 118 (2010) 670.
- [42]. Y. Y. Yeung, C. Rudowicz, J. Comput. Phys. 109(1993) 150.
- [43]. Y. Y. Yeung, C. Rudowicz, Comput. Chem. 16 (1992) 207.

Declarations

Ethical Approval:

This research did not contain any studies involving animal or human participants, nor did it take place on any private or protected areas. No specific permissions were required for corresponding locations.

Competing interests:

The authors declare that they have no known competing financial interests or personal relationships that could have appeared to influence the work reported in this paper.

Authors' contributions:

Maroj Bharati and Vikram Singh- performed calculations, wrote the manuscript and prepared the figure.
Ram Kripal- idea and supervision.
All authors have reviewed the manuscript.

Funding:

No funding is received.

Availability of data and materials:

The data will be made available on request.